# Application of Molodensky's Method for Precise Determination of Geoid in Iran

## Research article

Makan Abdollahzadeh<sup>1,2\*</sup> and Mehdi Najafi Alamdari<sup>2†</sup>

<sup>1</sup> Division of Geodesy and Geoinformatics, Royal Institute of Technology, Stockholm, Sweden <sup>2</sup> Faculty of Geodesy and Geomatics Engineering, K.N.Toosi University of Technology, Tehran, Iran

#### Abstract:

Determination of the geoid with a high accuracy is a challenging task among geodesists. Its precise determination is usually carried out by combining a global geopotential model with terrestrial gravity anomalies measured in the region of interest along with some topographic information. In this paper, Molodensky's approach is used for precise determination of height anomaly. To do this, optimum combination of global geopotential models with the validated terrestrial surface gravity anomalies and some deterministic modification schemes are investigated. Special attention is paid on the strict modelling of the geoidal height and height anomaly difference. The accuracy of the determined geoid is tested on the 513 points of Iranian height network the geoidal height of which are determined by the GPS observations.

#### Keywords:

Molodensky • Geoidal height and height anomaly • Iran

© Versita Warsaw and Springer-Verlag Berlin Heidelberg

Received 2011-03-17; accepted 2011-05-23

#### 1. Introduction

The recent developments in precise measurements of terrestrial gravity data and extra-terrestrial observations have made it possible to determine high-resolution and accurate solutions to the geodetic boundary value problems (GBVP). The geoid as a solution of the GBVP has an essential role in precise geodesy such as GPS-levelling as well as in geophysics. The Stokes and Molodensky formulas are two by-products of the GBVP providing the geoidal height and height anomaly respectively.

There are many researchers who employed Stokes' approach for the geoid determination, see e.g., Ellmann and Vaníček (2007), Sjöberg (2003a), Vaníček and Kleusberg (1987). In this approach, the terrestrial gravity observations must be downward continued to sea level considering the gravity effects of topographic masses. To do that, the mass distributions inside the topography must be known. In addition, the computational methods for downward continuation of the terrestrial gravities are another challenging task, e.g., in, Huang and Véronneau (2005), Martinec (1996), Moritz (1980), Vaníček et al. (1996).

In order to avoid the removal of the topographic masses, Molodensky et al. (1962) selected the Earth's surface, instead of the geoid, as the boundary to solve the Laplace second order differential equation for the height anomaly. In comparison with Stokes' method, there is no need to reduce the gravity observations from the Earth's surface down to the geoid (i.e., to the Earth's interior). The height anomaly, however, can be converted to the geoidal height by downward continuation. The main purpose of this paper is to explain a procedure for precise determination of the height anomaly based on a linearized simple Molodensky problem and a strategy for converting the height anomaly to the geoidal height.

During the past two decades, some well-known approaches were applied to compute the geoid models of Iran. Weber and Zommor-

<sup>\*</sup>E-mail: makan.abdollahzadeh@gmail.com

<sup>&</sup>lt;sup>†</sup>E-mail: mnajalm@yahoo.com

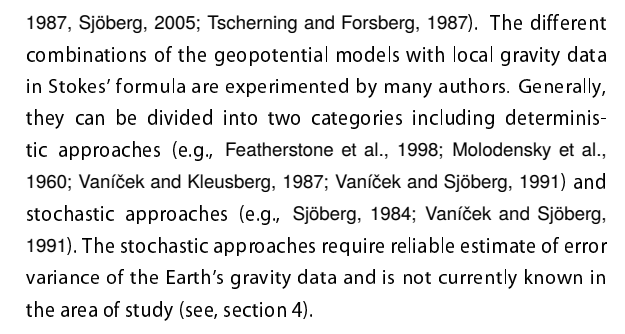
rodian (1988) were the first to compute such a model in Iran. Their method was based on the GPM2 geopotential model tailored with regional gravity data. Hamesh and Zommorrodian (1992) applied the remove-compute-restore technique along with the classical Stokes's formula for the geoid computation. The testing of this model using 200 GPS-levelling points showed an error of  $\pm 114$ cm. Najafi (2004) employed the Stokes-Helmert scheme (Vaníček et al., 1995) for the central part of Iran. Kiamehr and Sjöberg (2005a) assessed the accuracy of this model and showed a standard deviation of  $\pm 1.32$  m using 22 GPS-levelling data. In 2005, Safari et al. (2005) computed another geoid model based on a new ellipsoidal boundary value problem (Grafarend et al., 1999) and found an accuracy of  $\pm 1.06$  m in 51 GPS-levelling stations along the first-order levelling network of Iran. In another effort, Kiamehr (2006) used the KTH approach (Sjöberg, 2003a,b,c) for computation of a new geoid model. This model showed better accuracy than the previous models as the absolute error fit with 260 GPS-levelling data was 0.58 m.

In section 2, Molodensky's solution to GBVP and the procedure for precise determination of the height anomaly are briefly outlined. The geoidal height and height anomaly difference is formulated in section 3, while the numerical investigations are the subject of section 4. Finally, the paper concludes with the discussion of the outcomes in section 5.

## 2. Molodensky's solution and precise determination of the height anomaly

Molodensky's solution to modern geodetic boundary value problem leads to Fredohlm's integral equations of the second type. Its solution can be obtained iteratively and may be expressed as Stokes' formula after employing some approximations. This expression can be successfully applied in the remove-computerestore technique in conjunction with different methods of kernel modification. In zero approximation, the derived disturbing potential under an assumption of a spherical shape of the telluroid coincides with Stokes' solution (1849) to classical geodetic boundary value problem. However, in this approximation the effects of topographic variations are ignored so that the additive  $G_1$  and  $G_2$  corrections are taken into account by considering the height differences and inclination of the telluroid. The corresponding contributions of these additive terms to disturbing potential are computed utilizing Stokes' formula. The disturbing potential can be then converted to the height anomaly by use of the well-known Bruns formula.

With the recent dedicated gravimetric and gradiometric satellite missions of CHAMP, GRACE and GOCE, the accuracy of regional geoid/quasi-geoid have been highly improved. The combination of a satellite derived geopotential model, e.g., EIGEN-GL05S (Förste et al., 2008) with local gravity data is the most well-known approach for a regional gravimetric geoid/quasi-geoid determination (see, e.g., Forsberg, 1998; Sideris, 1990; Sideris and Schwarz;



The basic formulation of the remove-compute-restore technique for Molodensky's solution of the height anomaly can be written by:

$$\zeta_P = \zeta_M + \zeta_0^M + \zeta_{G_1}^M + \zeta_{G_2}^M \tag{1}$$

where  $\zeta_M$  is the portion of height anomaly determined from a global geopotential model up to degree M,  $\zeta_0^M$  is zero approximation of height anomaly from integration of residual terrestrial gravity anomalies  $\Delta g^M$ ,  $\zeta_{G_1}^M$  and  $\zeta_{G_2}^M$  are higher approximations of height anomaly or contributions of the Molodensky  $G_1$  and  $G_2$  terms. In geodetic literature Eq. (1) is called Molodensky's series and it converges only when the terrain inclination angle is less than 45° (Moritz, 1980; Ch.48), i.e., convergence of series cannot be guaranteed if the grid spacing of gravity anomalies is too small in rugged areas (Li et al., 1995).

The global geopotential models (GGM) have the most contribution to the geoidal height and height anomaly (see, Table 2). Over the past two decades, several GGMs were presented from the dedicated satellite gravity field missions (see, e.g., http://icgem.gfz-potsdam.de/ICGEM/ICGEM.html). Applying different strategies and observation time span for satellite data processing make their accuracies different from each other. It is well-known that the published error estimate for any GGM is global and not necessarily representative of its performance in a particular region. Therefore, as a first step in precise determination of the height anomaly we should investigate the accuracy of the GGMs in the area of interest. The standard way is to compare the GPS-levelling geoidal height and the particular GGM geoid. Kiamehr and Sjöberg (2005b) investigated the absolute and relative accuracy of some combined and satellite only GGMs versus 260 GPS-levelling points in Iran. However, our research study focuses on satellite only models which they are in high demand for the regional gravimetric geoid determination (see, e.g., Ellmann and Vaníček, 2007). The numerical results in Table 1 reveal that the geopotential model EIGEN-GL05S from the GRACE and LAGEOS missions fits the 513 GPS-levelling points of Iran with the best absolute accuracy among the GGMs such as ITG-Grace 2010S (Mayer-Gürr et al., 2010), AIUB-GRACE02S (Jäggi et al., 2009) and GGM03S (Tapley et al., 2007).

The high-frequency components of the height anomaly are given by convolution of the residual gravity anomalies and  $G_1$  and  $G_2$  terms with Stokes' function. The residual gravity anomalies  $\Delta g^M$ 

are obtained by subtracting the GGM anomalies  $\Delta g_M$  from the observed free-air gravity anomalies  $\Delta q_{FA}$ :

$$\Delta q^M = \Delta q_{FA} - \Delta q_M \tag{2}$$

The high frequency Stokes integration can be numerically evaluated using a quadrature based summation. In compensation for the incomplete coverage of terrestrial gravity data on the Earth, the modified kernel of integration relevant to a partial integration zone of spherical radius  $\psi_0$  is substituted for the original Stokes integration over the full solid angle. We can split the integration zone into three parts: contribution of the computation point itself  $\zeta_{0\bullet}^M$ ; the rest of the integration cap  $\zeta_{0\circ}^M$ ; and the contribution of farzones  $\zeta_{0\circ}^M$  (Novák et al., 2001):

$$\zeta_{0}^{M}(P) = \zeta_{0_{\bullet}}^{M} + \zeta_{0_{\odot}}^{M} + \zeta_{0_{\oplus}}^{M} 
= -\frac{R\Delta g^{M}(P)}{2\gamma_{P'}} Q_{0}^{M}(\psi_{0}) + \frac{R}{4\pi\gamma_{P'}} \sum_{Q}^{K} \left(\Delta g^{M}(Q) - \Delta g^{M}(P)\right) 
S^{M}(\psi_{Q}, \psi_{0}) \Delta\Omega_{Q} + \frac{R}{2\gamma_{P'}} \sum_{n=M+1}^{n_{max}} Q_{n}^{M}(\psi_{0}) \Delta g_{n}(P)$$
(3)

where R is the mean Earth's radius, the subscripts P and Q refer to the computation and integration points, respectively,  $\psi_0$  defines the integration radius of spherical cap for Stokes' integral,  $\psi_Q$  denotes the spherical distance between the computation point and the center of the Q-th cell,  $\Delta\Omega_Q$  is the surface area of integration element, K is the number of cells within the spherical cap and  $\gamma_{P'}$  is the normal gravity at point P' on telluroid. The function  $S^M(\psi_Q,\psi_0)$  in Eq. (3) is the modified Stokes kernel, and  $Q_n^M(\psi_0)$  is the truncation coefficients corresponding to the modified kernel.

Applying a modification of Stokes' kernel not only reduces the truncation error, but also attenuates the low-frequency errors more likely contaminated in the high frequencies of terrestrial gravity data  $\Delta q^M$ , (Vaníček and Featherstone, 1998). It is known that terrestrial gravity anomalies are influenced by variety of systematic effects such as biases in the base gravity, uncertainties in horizontal and vertical datum as well as inconsistencies in the type of height system and approximation errors due to use of a simplified free-air reduction formula. According to Vaníček and Featherstone (1998) the spheroidal kernel (the kernel referring to a low frequency spheroid) attenuates these errors to a greater extent than the modified types and yields preferable high-pass filter properties to low-frequency errors of terrestrial data. Hence, although the truncation error are minimized in modified kernel, the amount of leakage of low-frequency errors from the terrestrial gravity data into the solution is more than that when using the spheroidal Stokes kernel. However, Owing to the spatially varying error characteristic of the gravity anomalies, different results are usually expected in different areas.

The height anomaly obtained by Eq. (3) is improved by applying two corrective terms - the so called  $G_1$  and  $G_2$  terms. The  $G_1$  term presents the effects of irregularities of the Earth's topography which is expressed by Molodensky et al. (1962) as:

$$G_{1}(P) = \frac{R^{2}}{2\pi} \iint_{\sigma} \frac{H(Q) - H(P)}{l_{0}^{3}(\psi_{Q}, \psi_{1})} \left( \Delta g(Q) + \frac{3\gamma_{P'}(Q)}{2R} \zeta_{0}(Q) \right) d\sigma$$
(4)

where H(Q) and H(P) are the Molodensky normal height of the integration and computation points,  $l_0(\psi_Q,\psi_1)$  stands for the spherical distance between the computation point and the integration point and  $\psi_1$  is the radius of spherical cap for  $G_1$  integral. By applying the high frequencies of gravity anomalies  $\Delta g^M$  and height anomalies  $\zeta_0^M$  one can compute  $G_1^M$  and its corresponding contribution to the height anomaly from Stokes's integral. The contribution of computation point, rest of cap and the distance zone read:

$$\zeta_{1}^{M}(P) = \zeta_{1_{\bullet}}^{M} + \zeta_{1_{\odot}}^{M} + \zeta_{1_{\oplus}}^{M} =$$

$$-\frac{RG_{1}^{M}(P)}{2\gamma_{P'}}Q_{0}^{M}(\psi_{0}) + \frac{R}{4\pi\gamma_{P'}}\sum_{Q}^{K}\left(G_{1}^{M}(Q) - G_{1}^{M}(P)\right)$$

$$S^{M}(\psi_{Q}, \psi_{0})\Delta\Omega_{Q} + \frac{R}{2\gamma_{P'}}\sum_{n=M+1}^{n_{\max}}Q_{n}^{M}(\psi_{0})G_{1_{n}}(P)$$
(5)

where  $n_{max}$  is the maximum harmonic degree for computation of truncation error from a GGM and  $G_{1_n}$  is n-th harmonic in expansion of  $G_1$  term into spherical harmonics given by Heiskanen and Moritz (1967).

In  $G_2$  term, the second power of height differences and inclination of telluroid to reference ellipsoid  $\beta$  are considered and the integration is performed within the spherical cap of radius  $\psi_2$  (ibid):

$$G_{2}(P) = \frac{R^{2}}{2\pi} \iint_{\sigma} \frac{H(Q) - H(P)}{l_{0}^{3}(\psi_{Q}, \psi_{2})} \left( G_{1}(Q) + \frac{3\gamma_{P'}(Q)}{2R} \zeta_{1}(Q) \right) d\sigma$$

$$- \frac{3R}{8\pi} \iint_{\sigma} \frac{(H(Q) - H(P))^{2}}{l_{0}^{3}(\psi_{Q}, \psi_{2})} \left( \Delta g(Q) + \frac{3\gamma_{P'}(Q)}{2R} \zeta_{0}(Q) \right) d\sigma$$

$$+ \left( \Delta g(P) + \frac{3\gamma_{P'}(P)}{2R} \zeta_{0}(P) \right) \tan^{2} \beta_{P}$$
(6)

As a matter of fact,  $\beta$  is an angle between normal to telluroid (approximately normal to the Earth's surface) and the reference ellipsoid. It can be approximated by inclination of the Earth's surface in meridian and prime vertical planes, i.e.,

$$\tan^2 \beta_P \cong \left(\frac{\partial h_P}{\partial x}\right)^2 + \left(\frac{\partial h_P}{\partial y}\right)^2 = \tan^2 \beta_{x_P} + \tan^2 \beta_{y_P} \quad (7)$$

where the above relation expresses the maximum inclination of the Earth' surface as function of gradients at West-East and North-South directions. Using a grid-based DEM, one of the most common approaches is to use a moving  $3\times3$  window to derive finite differential or local surface fit polynomial for the calculation. Zhou and Liu (2004) studied six popular algorithms of finite differential for analysis of errors of derived slope from DEM. However, in our numerical studies we observed that applying different algorithms causes small discrepancies in  $G_2$  term, i.e., the maximum differences reach below 200  $\mu$ Gal level. The reasons are probably because of using a smoothed DEM, i.e., a grid of 5°×5° and remove-compute-restore technique which smooths the gravity and height anomalies.

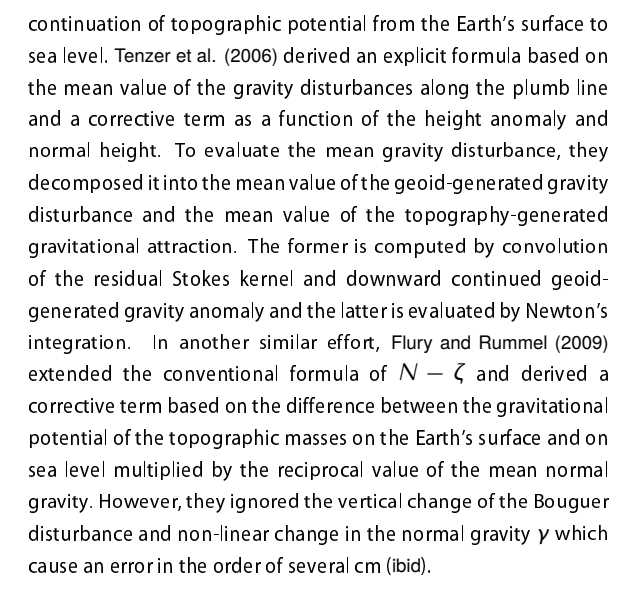
Again correction to the height anomaly is computed from Stokes' formula by splitting the integration zone to the computation point and rest of cap:

$$\begin{split} \zeta_{2}^{M}(P) &= \zeta_{2\bullet}^{M} + \zeta_{2\circ}^{M} = -\frac{RG_{2}^{M}(P)}{2\gamma_{P'}}Q_{0}^{M}(\psi_{0}) + \frac{R}{4\pi\gamma_{P'}}\\ \sum_{Q}^{K} \left(G_{2}^{M}(Q) - G_{2}^{M}(P)\right)S^{M}(\psi_{Q}, \psi_{0})\Delta\Omega_{Q} - \frac{R^{2}}{4\pi\gamma_{P'}}\sum_{Q}^{N}\\ \left[\frac{(H(Q) - H(P))^{2}}{l_{0}^{3}(\psi_{Q}, \psi_{4})}\left(\Delta g^{M}(Q) + \frac{3\gamma_{P'}(Q)}{2R}\zeta_{0}^{M}(Q)\right)\right]\Delta\Omega_{Q} \end{split} \tag{8}$$

The numerical evaluation of  $\zeta_2^M$  shows that it varies between -2 cm and +1 cm in Iran, see e.g., Table 2. Therefore, we expect a small truncation error in Eq. (8). The magnitude of the third constituent on the most right hand side of Eq. (8) is between -13 mm and +14 mm which should be considered for precise determination of the height anomaly. In this term  $\psi_4$  refers to integration radius of spherical cap.

#### 3. Geoidal height and height anomaly difference

The geoidal height and height anomaly difference, equivalently to the difference between normal and orthometric heights, is approximated using the conventional formula: the simple Bouguer anomaly times the topographic height divided by the normal gravity (Heiskanen and Moritz, 1967). However, this formula suffers from some assumptions made on the evaluation of mean value of the gravity along the plumb line. For instance, applying the Poincaré-Prey reduction for determining the gravity inside the topography with constant density as well as approximating the vertical gradient of gravity with the normal gradient yield even decimeter errors in the value of the geoidal height and height anomaly difference. Sjöberg (1995) slightly improved the formula by considering a small term related to the vertical derivative of the gravity anomaly. But it was concluded that his approximation might be insufficient in mountainous regions. Later on, Sjöberg (2006) presented an improved formula including corrective terms due to roughness of the topography and lateral variations of topographic mass density and a term related with the downward



In this research we derive a strict expression based on the mathematical formulas of the geoidal height and height anomaly. Our formula is very similar to that of Sjöberg (2006) but with a more rigorous derivation. To begin with, according to Vaníček et al. (2004) we work on the No-Topography gravity space (NT-space). In the NT-space, the gravitational attractions of topographic masses are removed before hand. Denoting the disturbing potential  $T_P$  at point P on the Earth's surface in the real space, and  $T_P^{NT}$  being the disturbing potential at the same point in NT-space, the following relation holds:

$$T_P^{NT} = T_P - V_P^T \tag{9}$$

where  $V_P^T$  are Newtonian volume integral for the gravitational potential by topographic masses. It is well-known that due to weak singularity of Newton's integral at computation point,  $V_P^T$  is decomposed into the effects of the spherical shell  $V_P^{T.S}$  and the roughness term  $V_P^{T.R}$  (see, e.g., Martineo, 1998):

$$V_{P}^{T} = V_{P}^{T.S} + V_{P}^{T.R} \tag{10}$$

Disregarding the ellipsoidal correction, the gravity anomaly  $\Delta g_P$  on the Earth's surface is expressed by the well-known relation, the fundamental formula of physical geodesy:

$$\Delta g_P \stackrel{\sim}{=} -\frac{\partial T}{\partial r}|_P - \frac{2}{r_P}T_P \tag{11}$$

Applying Eq. (11) to NT-space where inserting Eq. (9) into Eq. (11) the relation between real gravity anomaly and NT gravity anomaly (geoid-generated gravity anomaly) becomes:

$$\Delta g_P^{NT} \cong \Delta g_P + \frac{\partial V^T}{\partial r} |_P + \frac{2}{r_P} V_P^T$$
 (12)



where the second term on the right-hand side of the equation represents the direct topographic effects and the third term stands for the secondary indirect topographic effects on gravity. The mathematical formulas of direct and secondary indirect topographic effects can be found in geodetic literature (see, e.g., Vaníček et al. 2004). Now, by noting that the NT disturbing potential is harmonic everywhere outside the geoid, the Poisson integral equation as the solution of Dirichlet's boundary value problem can be used for upward/downward continuation of NT gravity anomaly:

$$\Delta g_P^{NT} = \frac{R^2}{4\pi r_P} \iint_{\sigma} \frac{r_P^2 - R^2}{L^3(r_P, \psi, R)} \Delta g_Q^{NT*} d\sigma \qquad (13)$$

where  $\Delta g^{NT*}$  is the gravity anomaly on the geoid. Eq. (13) shows that the gravity anomaly on the Earth's surface can be obtained from a linear combination of geoid-generated gravity anomalies on the geoid. Practically, in the case of downward continuation, the discrete inverse operation to the Poisson integral is applied and the NT gravity anomaly is downward continued to the geoid. Now, the geoidal height is determined from downward continued NT gravity anomalies and Stokes' formula applies:

$$N_{P} = \frac{R}{4\pi \gamma_{P_{0}^{\prime}}} \iint_{\sigma} \Delta g_{Q}^{NT*} S(\psi) d\sigma + \frac{V_{P_{0}^{\prime}}^{T}}{\gamma_{P_{0}^{\prime}}}$$
(14)

where  $\gamma_{P_0}$ ' denotes the normal gravity on the reference ellipsoid and  $V_{P_0}^T$  refer to the topographic potential on the geoid. Transformation of the real space to the NT-space, i.e., using  $\Delta g^{NT*}$  makes Stokes' formula to compute a co-geoid rather than the geoid. But addition of indirect effects computed by the second term in the right hand side of Eq. (14) changes the co-geoid back to the geoidal height  $N_P$ .

Equivalently, according to Heiskanen and Moritz (1967, Eq. 8-96), the extended Stokes formula for evaluation of the disturbing potential on the Earth's surface and consequently for the determination of the height anomaly can be used:

$$\zeta_{P} = \frac{R}{4\pi\gamma_{P'}} \iint_{\sigma} \Delta g_{Q}^{NT*} S(r_{Q}, \psi) d\sigma + \frac{V_{P}^{T}}{\gamma_{P'}}$$
 (15)

where  $S(r_Q,\psi)$  is the extended Stokes kernel and  $\gamma_{P'}$  is normal gravity on the telluroid. According to Eq. (15) the height anomaly can be alternatively determined from downward continuation of NT gravity anomalies and the indirect effects given by the topographic potential at point P on the Earth's surface. Now by subtracting Eq. (15) from Eq. (14), one obtains:

$$(N - \zeta)_{P} = \frac{R}{4\pi\gamma_{P'_{0}}} \iint_{\sigma} \Delta g_{Q}^{NT*} \left( S(\psi) - S(r_{Q}, \psi) \right) d\sigma$$
$$+ \frac{1}{\gamma_{P'_{0}}} \left( V_{P_{0}}^{T} - V_{P}^{T} \right) + d\zeta_{P}$$

$$(16)$$

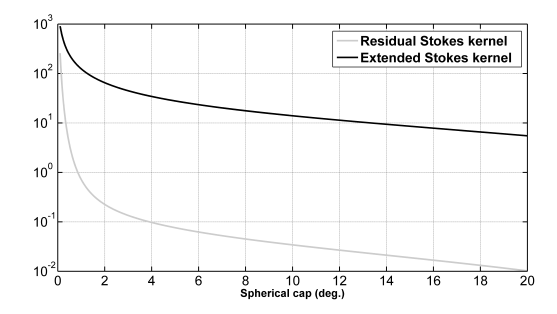


Figure 1. Extended  $S(r, \psi)$  and residual  $\Delta S(r, \psi)$  Stokes kernel for different spherical caps r = R + 9 km

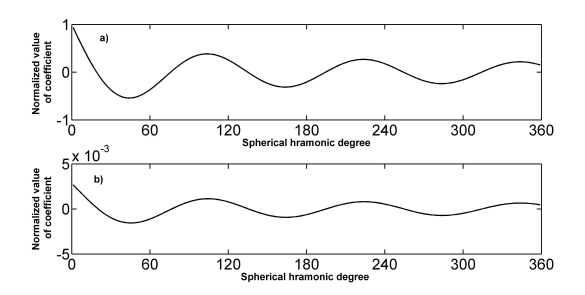


Figure 2. Normalized truncation coefficients, a) for the extended Stokes kernel  $S(r,3^\circ)$  b) for the residual Stokes kernel  $\Delta S(r,3^\circ)$ ; r=R+9 km

where the small correction  $d\zeta_P$  is given:

$$d\zeta_P = \zeta_P \left( \frac{\gamma_{P'}}{\gamma_{P'_0}} - 1 \right) \tag{17}$$

Equation (16) is the main formula for the geoidal height and height anomaly difference computation. According to the formula, the surface gravity anomaly should be transformed into the NT-space by removal of the whole masses above the geoid and then continued downward to the sea level by using the inverse Poisson integral. Applying the so-called residual Stokes integral, the first term on the right-hand side of Eq. (16), the values of  $N-\zeta$  are determined in the NT-space. Now we return to real space by adding the so-called residual indirect effects. The formula (16) is very similar to that of Tenzer et al. (2006) but was derived based on the mathematical formulas of the geoidal height and height anomaly.

Fig. 1 presents a comparison between the values of the residual Stokes kernel  $\Delta S(r,\psi)$  as a function of the spherical radius  $\psi$  and the geocentric distance r, and extended Stokes kernel  $S(r,\psi)$ . It shows that the residual kernel in an extreme case (r=R+9 km) approaches more rapidly to zero than the other kernels. Therefore, selection of a small integration radius can be efficient for numerical evaluation of the integral formula in Eq. (16). Accordingly, Fig. 2

shows the numerical value of the truncation coefficients  $Q_n(r,\psi^\circ)$  and  $\Delta Q_n(r,\psi^\circ)$  for the extended and residual Stokes kernels, respectively. For the comparison to be more clear, the coefficients have been normalized by multiplications of (n-1)/2, which is the inverse norm of Stokes' kernel. The value of r=9 km and  $\psi_0=3^\circ$  have been chosen to show an extreme case of the coefficients behaviour. An important point to observe from Fig. 2 is that the truncation error is greatly reduced in the residual Stokes integral because  $\Delta Q_n(r,\psi^\circ) < Q_n(r,\psi^\circ)$ . Thus, no modification to the residual Stokes kernel is necessary as the numerical value of the truncation error reaches a maximum value of 5 mm in the area of interest. Equivalently, the residual kernels in the evaluation of the residual topographic indirect effects are well-behaved, and in comparison with the original Newtonian kernel, they approach to zero faster.

It is well-known that in the Stokes-derived approaches for geoid determination, terrestrial gravity observations must be reduced for the effects of topographic masses and then be downward continued to a boundary surface through an unstable procedure (see, e.g., Ellmann and Vaníček, 2007; Kiamehr, 2006). A number of reduction methods have been proposed for this purpose which requires the mass density distributions between the geoid and Earth's surface to be known. In contrast, Molodensky's approach to the gravimetric boundary value problem results in the height anomaly, avoiding any gravity reduction and downward continuation procedures. However, through the height anomaly to geoidal height conversion, modelling the masses above geoid and downward continuation of gravity anomaly is unavoidable. It is appropriate to note that the main advantage of this approach for the determination of the geoid is that the effects of mass density variations and downward continuation of gravity anomaly enter indirectly so that they become smaller comparing to the classical Stokes idea. This can be easily seen from expression (16) where the residual kernels guarantee such reductions in residual Stokes integral and indirect effects. The effects of lateral mass density variations appear in the residual indirect effects and are expected to be small. It should be stated that these effects are very similar to the primary indirect topographic effects on the geoid through the Stokes-Helmert scheme for geoid determination. According to Huang et al. (2001) these effects reach a maximum of -2.5 cm over the Rocky Mountains. However, it should be noted that due to small effects of lateral density variations on the residual indirect effects we left the numerical evaluations to be undertaken in future work

The downward continuation effects of NT gravity anomaly can be computed for the geoidal height and height anomaly difference as below:

$$\delta(N - \zeta) = \frac{R}{4\pi\gamma_{P_Q'}} \iint_{\sigma} \left( \Delta g_Q^{NT*} - \Delta g_Q^{NT} \right) \Delta S(r_Q, \psi) d\sigma$$
(18)

From the numerical evaluation of Eq. (18), we found that the maximum absolute value of the effects of downward continuation



on  $N-\zeta$  reaches the 5 cm level over the rough areas in Iran (see, Fig. 5(b)). It is interesting to note that the downward continuation effects on the geoidal height in the Stokes-derived approaches are very noticeable as they approximately reach 1.6 m level in the same area (Kiamehr, 2006). However, these effects are significantly attenuated, i.e., up to 32 times, for the geoidal height and height anomaly conversion. Importantly, the leakage of the downward continuation-related errors to the geoidal height is reduced to a larger extend and they are attenuated by the residual Stokes kernel.

#### 4. Numerical investigations

- i) The 27,401 points of terrestrial and marine gravity data have been collected by different organizations using different gravimeters and methods during 70 years. Various kinds of systematic errors have affected the observations due to the uncertainty of reference frames and equipment. Therefore, a refinement process seems to be necessary prior to their use for geoid determination. Correlations of spatially distributed data can be used to detect gross errors (Tscherning, 1991). We interpolated the gravity value at each observation point in order to compare the observed value and the predicted one. If the difference is larger than a certain threshold then the observation is considered as blunder. The least-squares collocation is a well-proven interpolation method in geodetic science and can be successfully used for blunder removal (ibid). Instead, the Kriging interpolation technique was used, primarily because this is readily available in the gridding software such as Surfer software and is suited to interpolating the geoscience data. As a result, 7% of the available data were eliminated in the numerical process. Since the gravity data are only available within Iran, we used a very high degree geopotential model like EGM08 (Pavlis et al., 2008) to fill the gaps out of the border. This somewhat reduces the omission error in geoid model near the border of Iran. Furthermore, as a sea-surface data, the recently altimetrically determined gravity anomaly DNSC08GRA (Andersen et al., 2010) was used to fill out the region of the Persian Gulf and Oman Sea. Fig. 4(a) presents the distribution of the gravity data in Iranian territory. It can be seen that large areas suffer from poor number of observations.
- ii) The digital elevation models (DEMs) are mainly used for gridding of heterogeneous gravity data and evaluation of topographic effects through the geoid modelling procedures. There are several public DEMs with global coverages. Most of these models, in grid format, were generated based on the remote sensing techniques. The digital elevation model SRTM3 (Rodriguez et al., 2005) with resolution of 3 arc-second is the latest model based on satellite radar

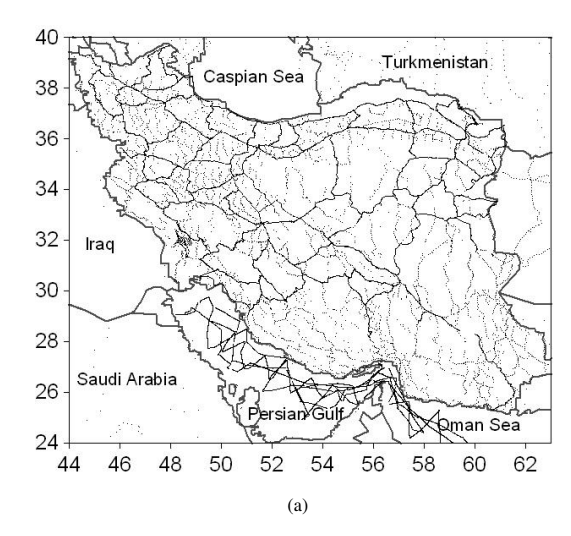
interferometry technique. Kiamehr (2005b) tested the accuracy of some global models using GPS-levelling data in Iran. According to that study, SRTM DEM with an estimated accuracy of 6.5 m is the best among the various tested DEMs. We therefore adopted SRTM DEM as our background model.

iii) Traditionally, absolute and relative external accuracy of the gravimetric regional geoid is evaluated by using GPS-levelling points. The total numbers of GPS-levelling available in Iran is 513 which most of points belong to secondand third-order levelling networks and a few of them are located in the first-order national network. It should be stated that systematic errors in the national levelling network like, neglecting the orthometric correction to levelling observations, systematic biases in definition of the vertical datum and etc, may affect the accuracy of GPS-levelling points. According to Kiamehr (2005) the spirit levelled heights are accurate at 0.7 m level. The geographic locations of GPS-levelling points are shown in Fig. 4(b).

As the first step, the validated heterogeneous gravity data were interpolated on 5'×5' geographic grid. Since gridding of free air gravity anomalies are subjected to aliasing effects they are usually reduced for topographic effects before gridding process. Among the methods of gravity reduction such as complete Bouguer model, residual terrain model (RTM) and isostatic reductions, we found that the isostatic reduction method of Airy-Heiskanen results in smoother gravity anomaly in the area of interest. In addition, we performed the geoid computations process for each reproduced free air gravity anomaly. The fit to GPS/leveling geoid was a criterion for our final decisions. In this respect, we reduced the free air gravity anomalies by using the isostatic Airy-Heiskanen model and EGM08 gravity anomaly. The reduced gravity anomalies were interpolated into the regular 5'×5' grid by using an arbitrary interpolator scheme such as Kriging and then the free air gravity anomalies obtained after restoring the topographic effects and EGM 08 contribution on the grid.

Table 1 gives the statistics properties of absolute comparison between the geoidal heights up to degree and order 150 derived from some of the recent GRACE-based GGMs and available GPS-levelling data. As can be seen, the EIGEN-GL05S gives superior result in terms of RMSE and therefore was regarded as a reference geopotential model in the computational process of height anomaly. It should be noted that at the time of this study, GOCE's GGMs were not available to the user community and we just used the GRACE models.

The height anomaly was determined based on the numerical evaluation of Eq. (1) corresponding to contribution of the geopotential model, terrestrial data,  $G_1$  and  $G_2$  terms. It was converted to the geoidal height using the method presented in section 3. The geoid solutions, computed using different spherical caps, maximum degree of modified kernels and geopotential model,



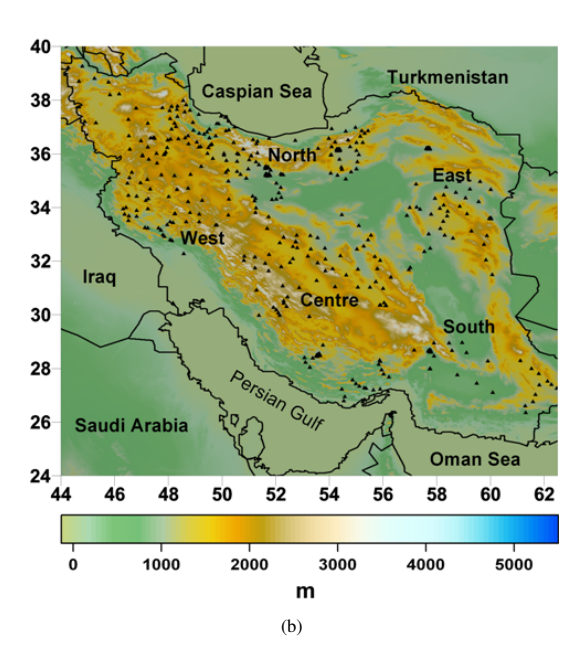


Figure 3. (a) Distribution of gravity data in Iran. (b) The 30" mean digital elevation model based on 3" SRTM data and distribution of GPS-levelling data. Location of five subzones for GPS-levelling data.

Table 1. Statistics for GGMs geoid comparison with GPS-levelling data. Unit: Metre.

Model	Max.	Min.	Mean	Std.	RMSE
ITG-Grace2010S	3.03	-3.80	-0.60	1.15	1.30
GGM03S	2.95	-3.49	-0.68	1.22	1.39
AIUB-GRACE02S	2.89	-3.65	-0.60	1.14	1.30
EIGEN-GL05S	3.50	-3.63	-0.56	1.14	1.26



were interpolated and compared with 513 GPS-levelling geoidal heights. According to our numerical experiments (not presented here), comparing with spheroidal kernel and Vaníček-Kluesberg modification, Featherstone scheme with degree of modification and geopotemtial model M = 100 and spherical cap  $\psi_0 = 1^\circ$ gives the best result. We noticed that the increasing degree of modification and geopotential model degrades the RMSE fit with the GPS-levelling geoidal height. This is expected due to growing the errors in satellite-derived geopotential models for the high harmonic degrees, e.g., for degrees higher than 130 the ratio of noise to signal reaches to 50 percent. It is noted that the RMSE fit degrades with increasing the spherical cap, e.g., for M = 100ranging from 1° to 3°. The main reason for such behaviour is the low quality of terrestrial gravity data in Iran which would allow more leakages of errors to occur into the geoid for large spherical cap.

Now by adopting the Featherstone scheme for modification of Stokes' kernel, we present more details about the numerical evaluation of integral formulas and their corresponding magnitudes. The important issue for the evaluation of the  $G_1$  and  $G_2$  terms is to select the proper integration radii. The numerical tests show that  $G_1$  and  $G_2$  terms evaluated from the integration caps 4° to 5° and  $1^{\circ}$  to  $2^{\circ}$  differ by less than 10  $\mu$ Gal in absolute values. Therefore, integration radii equal to  $4^{\circ}$  and  $2^{\circ}$  were used to evaluate  $G_1$ and  $G_2$  terms, respectively. In Table 2, the contributions of these two terms to the height anomaly are presented (see, Eq. (5) and Eq. (8)). It shows that the corrective term  $\zeta_1^{100}$  reaches a maximum of 19 cm over the mountainous area. Our numerical results revealed that the truncation error in evaluating of the  $\zeta_1^{100}$  term through the truncated Stokes formula (see, Eq. (5)) reaches the 3 cm level, which is considerable for a geoid accuracy on the 1 cm level. According to Table 2 we can also see that most contribution of the height anomaly is related to the geopotential model  $\zeta_{100}$ . This means that the planar approximation made on the solution of linearized simple Molodensky problem, which at most introduces 0.4% error (Moritz, 1980), is only concerned on the residual height anomaly through the remove-compute-restore technique.

From Table 2 we can also see that the values of  $\zeta_2^{100}$  minimally reaches the -2 cm level. It should be again emphasized that we used 5'×5' mean gravity anomalies for computing the height anomaly and geoidal height. According to Li. et al. (1995) a denser dataset can provide more details in rough mountainous areas. They reported on achieving significant improvement for the height anomaly prediction over the Canadian Rocky Mountains by using a grid spacing of 1 km by 1 km instead of 5'×5'. Indeed, it is expected to see more significant values for terms  $\zeta_1$  and  $\zeta_2$  using the finer grid spacing. However, this does not appear to be the case in Iran due to poor gravity data coverage, and makes it impossible to reach finer grid spacing.

Fig. 5(a) shows a plot of the computed  $N-\zeta$  values based on Eq. (16). As expected, the minimum value, which reaches -2.33 m, is connected with heights part of the Alborz Mountains. From

Table 2. Statistics for the height anomaly. Unit: Metre.

_1	parameter	Max.	Min.	Mean	Std.
	$\zeta_{100}$	34.48	-62.88	-13.69	19.93
	$\zeta_0^{100}$	4.07	-4.37	-0.03	0.71
	$\zeta_1^{100}$	0.19	-0.08	0.00	0.01
	$\zeta_{2}^{100}$	0.01	-0.02	0.00	0.00

Table 3. Statistics for the geoidal height and height anomaly difference. Unit: Metre.

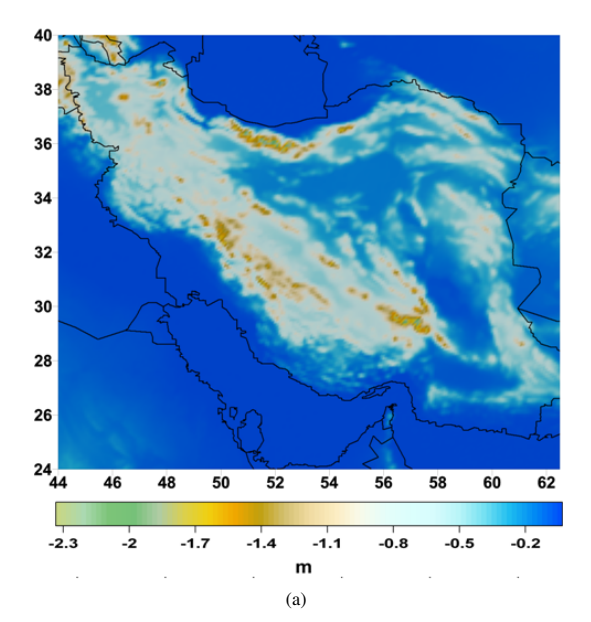
Parameter	Max.	Min.	Mean	Std.
Res. Stokes	0.07	-0.13	-0.00	0.01
Res. indirect	-0.03	-2.91	-0.29	0.33
$d\zeta$	0.02	-0.02	-0.00	0.00
Ν-ζ	-0.03	-2.33	-0.27	0.31

Table 3 we notice that the greatest contribution of  $N-\zeta$  is related to the residual indirect effect lying within the interval -2.91 to -0.03 m. Therefore, an optimal method for numerical integration is essential for accurate topographic roughness potential modelling. A complex investigation of this matter is still in progress and will be reported in the future. Similar to  $G_1$  and  $G_2$  terms, a numerical test was carried out for selecting a proper integration radius in evaluation of the residual Stokes integral. Consequently, a spherical cap of 3° was used to achieve mm accuracy. Prior to solving the residual Stokes integral, the surface gravity anomalies were transferred to NT-space by using Eq. (12). The integral formulas for the direct and secondary indirect topographical effects were numerically evaluated over the integration domain divided into the far zone, near zone and inner zone. Different DEMs were used with resolution of 30" and 5' for the evaluation of inner zone and near zone with integration radius of spherical cap of 30' and 5°, respectively. A global DEM with 1° ×1° resolution was used for the integration over the remaining spherical cap or the far zone contribution. The downward continued NT gravity anomalies were computed by using numerical evaluation of the Poisson formula with integration radius 80 $^{\circ}$ . The numerical estimate of Eq. (18)reveals that the downward continuation effcets of NT gravity anomaly on the geoidal height and height anomaly difference varies between -5.3 cm and 2.8 cm. A plot of these values is illustrated in Fig. 5(b).

By way of comparison, the geoid model based on the presented strategy for  $N-\zeta$  and conventional method was compared with the 49 GPS-levelling geoidal heights located in rough mountainous areas, i.e., in an area with more than 2000 m in height. It was observed that our technique improves the RMSE fit of geoid up to  $\pm$ 14 cm with respect to conventional method.

Fig. 5 presents the geoid model for Iran computed based on the Molodensky's approach and the presented technique for convert-





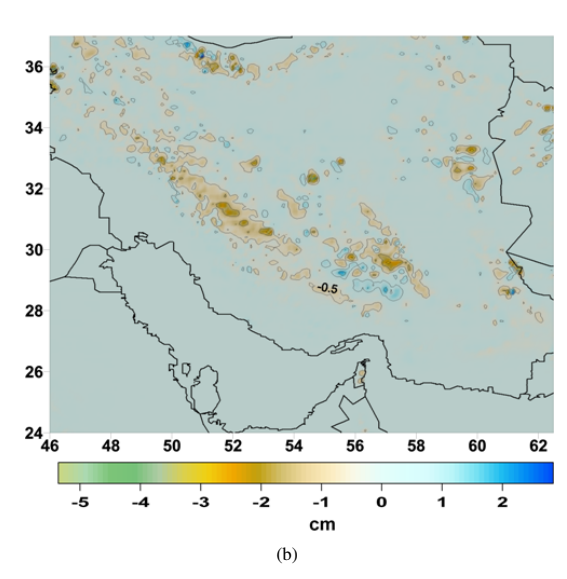


Figure 4. (a) Geoidal height and height anomaly difference  $N-\zeta$ . Unit: Metre (b) Downward continuation effects of NT gravity anomaly on the geoidal height and height anomaly difference. Unit: Centimeter.

ing the height anomaly to geoidal height. The internal accuracy of the geoid can be evaluated by propagating the errors of the source data into the result. The reliability depends on how realistic the source data errors are. However, we left such assessment for the future because there is no reliable estimate for the error of the gravity and height data. As was mentioned before, the external accuracy of the geoid is verified using GPS-levelling geoidal heights in absolute and relative sense. In the absolute verification, the external accuracy is achieved by comparing the gravimetric

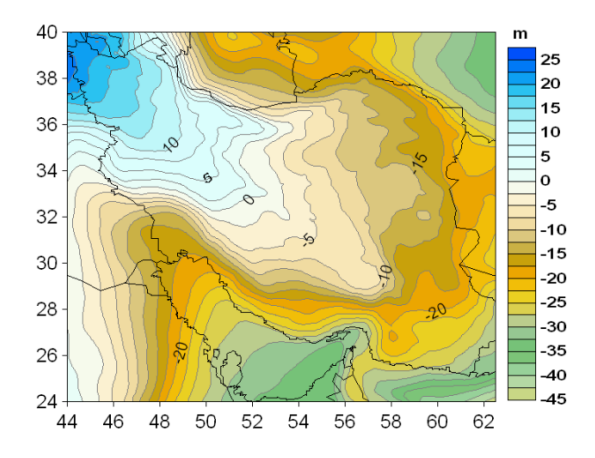


Figure 5. Gravimetric geoid model for Iran. Unit: Metre.

Table 4. Statistics for new geoid model absolute and relative comparison with GPS-levelling data, Unit: Metre.

Parameter	No. points.	Max.	Min.	Mean	RMSE	ppm
New Geoid	-	24.55	-43.84	-12.39	13.08(Std)	-
Abs.	513	1.41	-1.72	-0.05	0.53	-
North	74	2.05	-2.45	0.04	0.61	4.30
East	32	1.38	-1.05	0.14	0.49	3.60
South	38	1.49	-1.54	-0.12	0.50	1.95
West	34	0.62	-0.95	-0.22	0.38	2.77
Centre	35	1.91	-2.13	-0.02	0.65	4.05

geoid with GPS-levelling derived geoid. The grid of gravimetric geoid was interpolated to the position of GPS stations based on a gridding scheme such as Kriging. We note that the problems of selecting a suitable interpolation scheme are out of scope of this paper and left for future.

To take the assessment of external accuracy further, the gravimetric geoid was verified in relative sense. In this case, the difference in orthometric height is subtracted from the difference in the ellipsoidal height to give gradient over specific baselines. The main benefit of this method is that it removes systematic errors. For instance, vertical datum-related errors are noticeably reduced, especially over short baselines. In order to avoid long baselines, we verified the relative accuracy of the new geoid model in five subzones as illustrated in Fig. 4(b). The relative differences were computed over all the possible baselines between GPS stations. The results are summarized in Table 4.

The differences in absolute values of the geoidal heights are 1.41 m maximum, -1.72 m minimum and  $\pm 53$  cm RMSE on 513 GPS-levelling points. The relative RMSE vary from  $\pm 38$  cm in the West zone to  $\pm 65$  cm in Central zone. The relative difference can be expressed in parts per million (ppms) upon division with the baseline length. The mean values of the relative differences

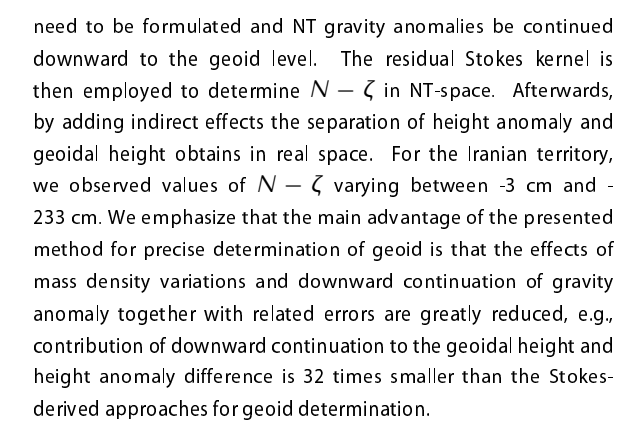
over each zone are shown in Table 4. As expected, the minimum relative differences are observed over the Southern area and it increases when moving towards the North of the country. Most likely, the main reason for such behaviour stems from increasing cumulative errors of spirit levelling from the zero point of the Iranian height system in the southern coastal areas. Furthermore, growing  $or thometric corrections to spirit | eve | | led \, data \, towards \, the \, Nor therm$ part and disregarding this correction will cause such discrepancies. Over the west zone, the gravimetric geoid model performs much better than other zones, partly because of the high density of gravity measurements. However, in rough areas like the Northern and Central zones, we observed larger discrepancies where our geoid model and GPS-levelling data include errors. Improper spatial coverage and quality of the terrestrial data, interpolation error of the free air gravity anomalies, instability of the downward continuation procedure and dicretization error in modelling of topographic effects as well as the planar approximation implied in solving of the simple Molodensky's problem are the main reasons for the low quality of gravimetric geoid model in these areas.

It is interesting to note that, the absolute RMSE fit of the EIGEN-GL05S geoid up to degree and order 100 with GPS-levelling data decreases by more than 65% in comparison with the new computed geoid, i.e., reduced from  $\pm 152\,\mathrm{cm}$  to  $\pm 53\,\mathrm{cm}$ . The gravimetric geoid model is usually fitted to the GPS-levelling data by four, five or seven parametric models to eliminate possible systematic errors in the geoid (Kotsakis and Sideris, 1999). However, In order to avoid the prolongation of the paper we do not consider such fitting procedure in our study. We note that detailed discussion on verifying the gravimetric geoid model and GPS-levelling data forms an entirely different scope of study.

#### 5. Summary and conclusions

This paper summarized the main theoretical principles of Molodensky's approach to precise determination of the height anomaly. The validated land and marine gravity data as well as the most recent geopotential model (EIGEN-GL05S from the GRACE and LAGEOS missions) and new digital elevation model (SRTM) were used in precise computation of the height anomaly. Comparing different deterministic approaches to modification of Stokes' kernel, we can say that in our experiment (not presented in the paper), Featherstone method gives the best result. In addition, the principles of selecting the appropriate modification degree and integration radius of spherical cap were revised and the values of M=100 and  $\psi_0=1^\circ$  were selected, respectively. We also conclude that aiming to compute the geoid accurate on 1 cm level, the truncation error for  $\zeta_1^{100}$  is significant as its magnitudes reached as much as 3 cm.

The relation between the height anomaly and geoidal height was modelled based on rigorous formula. To achieve  $N-\zeta$  in No-Topography space, the topographic effects on gravity anomalies



Finally the gravimetric geoid was evaluated by comparing the geoid with 513 GPS-levelling data in absolute and relative sense. An absolute agreement of  $\pm 53$  cm RMSE was determined. The relative investigations in five subzones across the country show the mean relative accuracy varying between 1.95 ppm and 4.30 ppm. The presented strategy shows its own efficiency comparing with the other tested methods in the area of study. The results are relevant for a number of geodetic applications. Further on, this model can be advantageous to future studies of geophysics and geodynamics in Iran.

#### Acknowledgment

The authors would like to express their gratitude to Dr. Mehdi Goli for numerical help. Dr. Mehdi Eshagh is appreciated for reading the manuscript. The unknown reviewers are cordially acknowledged for the constructive comments and their criticisms.

### References

Andersen B., Knudsen P., Berry P., 2010, The DNSC08GRA global marine gravity field from double retracked satellite altimetry, J. Geod., 84, 191-99.

Ellmann A., Vaníček P., 2007, UNP application of Stokes-Helmert's approach to geoid computation, J. Geodyn., 43, 200-213.

Featherstone W.E., Evans J.D., Olliver J.G., 1998, A Meissl-modified Vaníček and Kleusberg kernel to reduce the truncation error in gravimetric geoid computations. J. Geod., 72, 154-160.

Forsberg R., 1998, The use of spectral techniques in gravity field modelling: Trends and perspectives. Phys. Chem. Earth, 23, 31-39.

Flury J., Rummel R., 2009, On the geoid-quasigeoid separation in mountain areas, J. Geod., 83, 829-847.



Förste C., et al., 2008, A new global combined high-resolution GRACE-based gravity field model of the GFZ-GRGS cooperation, Geophysical Research Abstracts, A-03426, Vol. 10, EGU General Assembly 2008.

Grafarend E., Ardalan A.A., Sideris M.G., 1999, The spheroidal fixed-free two-boundary-value problem for geoid determination (the spheroidal Bruns transformation). J. of Geod., 73, 513-533.

Hamesh M., Zomorrodian H., 1992, Iranian gravimetric geoid determination-second step, NCC J. Surveying, 6, 52-63.

Heiskanen W.A., Moritz H., 1967, Physical geodesy, Freeman, San Francisco, 364 pp.

Huang J., Vaníček P., Pagiatakis S., Brink W., 2001, Effect of topographical mass density variation on gravity and geoid in the Canadian Rocky Mountains. J. Geod., 74, 805-815.

Huang J., Véronneau M., 2005, Applications of downward-continuation in gravimetric geoid modeling: case studies in Western Canada, J. Geod 79, 135-145.

Jäggi A., Beutler G., Meyer U., Prange L., Dach R., Mervart L., 2009, AlUB-GRACE02S-Status of GRACE Gravity Field Recovery using the Celestial Mechanics Approach, presented at the IAG Scientific Assembly 2009, August 31-September 4 2009, Buenos Aires, Argentina.

Kiamehr R., 2006, A strategy for determining the regional geoid by combining limited ground data with satellite-based global geopotential and topographical models: a case study of Iran. J. Geod., 79, 602-612.

Kiamehr R., Sjöberg L.E., 2005a, The qualities of Iranian gravimetric geoid models versus recent gravity field missions. Stud. Geophys. Geod., 49, 289-304.

Kiamehr R., Sjöberg L.E., 2005b, Effect of the SRTM global DEM on the determination of a high-resolution geoid model: a case study in Iran, J.Geod., 79, 540-551.

Kotsakis C., Sideris M.G., 1999, On the adjustment of combined GPS\_levelling/geoid networks. J. Geod., 73, 412-421.

Li Y.C., Sideris G., Schwarz K.P., 1995, A numerical investigation on height anomaly Prediction in mountain areas, Bulletin Géodésique, 69 ,143-156, 1995.

Martinec Z., 1996, Stability investigations of a discrete downward continuation problem for geoid determination in the Canadian Rocky Mountains. J. Geod., 70, 805-828.

Martinec Z., 1998, Boundary-Problems for Gravimetric Determination of a Precise Geoid, SpringerVerlagBerlinHeidelberg.

Molodensky M.S., Eremeev V.F., Yurkina M.I., 1962, Methods for study of the external gravitational field and figure of the Earth. Translated from Russian by the Israel program for scientific translations, Office of Technical Services Department of Commerce, Washington, D.C.

Moritz H., 1980, Advanced Physical Geodesy, Herbert Wichmann Verlag.

Mayer-Gürr T., Kurtenbach E., Eicker A., 2010, ITG-Grace2010: the new GRACE gravity field release computed in Bonn, Geophysical Research Abstracts, A-03426, Vol. 12, EGU2010-2446, EGU General Assembly 2010.

Najafi M., 2004, Determination of Precise geoid for Iran based on Stokes-Helmert Scheme. Report 2003, National Cartographic Center of Iran (NCC), TOTAK Project, Iran.

Novák P., Vaniček P., Véronneau M., Holmes S.A., Featherstone W.E., 2001, On the accuracy of modified Stokes's integration in high-frequency gravimetric geoid determination. J. Geod., 74, 644-654.

Pavlis N.K., Holmes S.A., Kenyon S.C., Factor J.K., 2008, An Earth gravitational model to degree 2160: EGM2008, Presented at the 2008 General Assembly of the European Geosciences Union, Vienna, Austria, April 13-18.

Rodriguez E., Morris C.S., Belz J.E., Chapin E.C., Martin J.M., Daffer W., Hensley S., 2005, An Assessment of the SRTM Topographic Products. Technical Report JPL D-31639, Jet Propulsion Laboratory, Pasadena, California.

Safari A., Ardalan A. A., Grafarend, E.W., 2005, A new ellipsoidal gravimetric, satellite altimetry, astronomic boundary value problem; case study: geoid of Iran. J. Geodyn., 39, 545-568.

Sideris M.G., 1990, Rigorous gravimetric terrain modelling using Molodensky's operator, Manuscr. Geod. 15:97-106.

Sideris M.G., Schwarz K.P., 1987, Improvement of medium and short wavelength features of geopotential solutions by local gravity data, Boll. Geod. Sci. Affini, Vol. XLVI, 207-221.

Sjöberg L.E., 1984, Least squares modification of Stokes' and Vening Meinesz' formulas by accounting for truncation and potential coefficient errors, Manuscr. Geod., 9, 209-229.



Sjöberg L.E., 1995, On quasigeoid to geoid separation, Manuscr. Geod, 20, 182-192.

Sjöberg L.E., 2003a, A computational scheme to model the geoid by the modified Stokes formula without gravity reductions. J. Geod., 74, 255-268.

Sjöberg L.E., 2003b, A general model of modifying Stokes' formula and its least squares solution. J. Geod., 77, 459-464.

Sjöberg L.E. 2003c, A solution to the downward continuation effect on the geoid determined by Stokes' formula. J Geod, 77, 94-100.

Sjöberg L.E., 2005, A discussion on the approximations made in the practical implementation of the remove-compute-restore technique in regional geoid modeling, J. Geod., 78, 645-653.

Sjöberg L.E., 2006, A refined conversion from normal height to orthometric height, Stud. Geophys. Geod., 50, 595-606.

Stokes G.G., 1849, On the variation of gravity on the surface of the Earth. Trans Camb Phil Soc 8: 672-695.

Tapley B., Ries J.,Bettadpur S., Chambers D., Cheng M., Condi F., Poole S. 2007, The GGM03 Mean Earth Gravity Model from GRACE, Eos Trans. AGU 88(52), Fall Meet. Suppl., Abstract G42A-03.

Tenzer R., Novák P., Moore P., Kuhn N., Vaníček P., 2006, Explicit formula for the geoid-quasigeoid separation, Stud. Geophys. Geod., 50, 607-618.

Tscherning C.C., 1991, The use of optimal estimation for gross-error detection in databases of spatially correlated data. BGI, Bulletin d' Information 68, 79-89.

Tscherning C.C., Forsberg R., 1987, Geoid determination in the Nordic countries from gravity and height data., Boll. Geod. Sci. Aff., 46, 21-43.

Vaníček P., Kleusberg A., 1987, The Canadian geoid-Stokesian approach. Manuscr. Geod, 12, 86-98.

Vaníček P., Sjöberg L.E., 1991, Reformulation of Stokes's theory for higher than second-degree reference field and modification of integration kernels. J. Geophysical Research-Solid Earth, 96, 6529-6539.

Vaníček P., Najafi M., Martinec Z., Harrie L., Sjöberg L.E., 1995, Higher degree reference field in the generalized Stokes-Helmert scheme for geoid computation. J. Geod., 70, 176-182

Vaníček P., Sun W., Ong P., Martinec Z., Najafi M., Vajda P. and TerHorst B., 1996, Downward continuation of Helmert's gravity anomaly. J. Geod., 71, 21-34.

Vaníček P., Featherstone W.E., 1998, Performance of three types of Stokes's kernel in the combined solution for the geoid, J. Geod., 72, 684-697.

Vaníček P., Tenzer R., Sjöberg L.E., Martinec Z., Featherstone W.E., 2004, New views of the spherical Bouguer gravity anomaly. Geophys. J. Int., 159, 460-472.

Weber G., Zomorrodian H., 1988, Regional geopotential model improvement for the regional Iranian geoid determination. Bulletin Géodésique, 62, 125-141.

Zhou Q., Liu X., 2004, Analysis of errors of derived slope and aspect related to DEM data properties, Computers & Geosciences, 30, 369-378.

